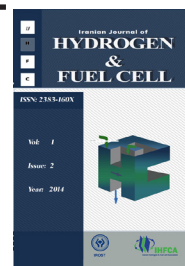


Iranian Journal of Hydrogen & Fuel Cell

IJHFC

Journal homepage://ijhfc.irost.ir



## Novel PVA/La<sub>2</sub>Ce<sub>2</sub>O<sub>7</sub> hybrid nanocomposite membranes for application in proton exchange membrane fuel cells

Khadijeh Hooshyari<sup>1,2</sup>, Mehran Javanbakht<sup>1,2,\*</sup>, Morteza Enhessari<sup>2</sup>, Hossein Beydaghi<sup>1,2</sup>

<sup>1</sup> Department of Chemistry, Amirkabir University of Technology, Tehran, Iran

<sup>2</sup> Renewable Energy Research Center, Amirkabir University of Technology, Tehran, Iran

### Article Information

Article History:

Received:

17 April 2014

Received in revised form:

6 August 2014

Accepted:

9 September 2014

### Keywords

PEM fuel cell

PVA (poly vinyl alcohol)

Nanocomposite membranes

Proton conductivity

### Abstract

Proton exchange membrane (PEM) fuel cells are electrochemical devices that show the highest power densities compared to the other types of fuel cells. In this work, nanocomposite membranes were used for proton exchange membrane fuel cells as poly(vinyl alcohol)/La<sub>2</sub>Ce<sub>2</sub>O<sub>7</sub> (PVA-LC) with the aim of increasing the water uptake and proton conductivity. Glutaraldehyde (GA) was used as cross linking agent of PVA matrix. PVA-LC nanocomposite membranes have been prepared with solutions casting method. The significant improvement has been achieved via the synergetic combination of organic and inorganic phases. Nanocomposite membranes were structurally, morphologically and electrochemically considered by FT-IR, SEM and EIS, respectively. The results exhibited that the proton conductivity and the water uptake of the nanocomposite membranes were higher than that of the PVA membrane. PVA-LC nanocomposite membranes containing 4 wt.% of La<sub>2</sub>Ce<sub>2</sub>O<sub>7</sub> nanoparticles displayed a high proton conductivity (0.019 S/cm). The highest peak power density of the PEM fuel cell using PVA-LC nanocomposite membrane at ambient temperature was 19 mW/cm<sup>2</sup>. The proposed PVA-LC nanocomposite membranes appear to be a viable candidate for future PEM fuel cells applications.

## 1. Introduction

Proton exchange membrane (PEM) fuel cells are electrochemical devices that show the highest power densities compared to the other types of fuel cells [1]. Polyperfluorosulfonic acid (PFSA) membranes such as Nafion are the most common electrolyte membranes used for PEM fuel cells due to their high proton

conductivity, good mechanical strength and excellent chemical and thermal stability. However, the high cost of Nafion and its instability at high temperatures delay its extensive applicability [2]. So, production of new proton conducting membranes to replace Nafion has been the subject of constant research. Poly (vinyl alcohol) (PVA) is a low cost polymer and has the exceptional characterizations of good chemical and

\*Corresponding author: Department of Chemistry, Amirkabir University of Technology, Tehran, Iran. Tel.: +98 2164542764; Fax: +9821 64542762.  
E-mail address: mehranjavanbakht@gmail.com (M. Javanbakht).

mechanical stability and dense reactive chemical functions favorable for cross-linking. PVA can be industrially produced; it is non-toxic and can easily form thin, large surface-area membranes characteristics most desired of fuel cells. Low proton conductivity and highly swelling of PVA membrane limit its usefulness as a proton exchange membrane [3]. Studies have shown that the addition of inorganic particles, due to high surface area, improves the water uptake and proton conductivity of PVA polymer electrolyte membranes, such as PVA/SiO<sub>2</sub>, PVA/TiO<sub>2</sub>, etc [4]. Preparation of the polymer/inorganic (nano) composites is another approach to improve the properties of these membranes. PVA/SiO<sub>2</sub>-PVA composite [5] and PVA/montmorillonite [6] nanocomposite membranes have been prepared. Development of new materials that are more stable and development of new additives which can improve the stability of existing materials are main principal strategies for commercialization of PEM fuel cells. The incorporation of hydrophilic inorganic metal oxide particles has produced promising results, because of their tendency to accommodate water and acid in their interlayer region and turn out to be more hydrophilic or more permeable to water.

Recently, we introduced new proton conducting hybrid membranes based on PVA, and nanoporous silica containing phenyl sulfonic acid [7] and poly(sulfonic acid)-grafted silica nanoparticles [8]. Newly, Nafion/Fe<sub>2</sub>TiO<sub>5</sub> nanocomposite membranes were prepared by dispersion of Fe<sub>2</sub>TiO<sub>5</sub> nanoparticles within the commercial Nafion membranes [9]. Incorporation of Fe<sub>2</sub>TiO<sub>5</sub> nanoparticles in Nafion matrix improved the thermal stability of Nafion membranes which is important for operating of PEM fuel cells at elevated temperatures. As we mentioned it seems that in Fe<sub>2</sub>TiO<sub>5</sub> nanoparticles when Fe<sup>3+</sup> cations are placed near Ti<sup>4+</sup> cations, the acidic character of these ions is increased.

La<sub>2</sub>Ce<sub>2</sub>O<sub>7</sub> nanoparticles have a cubic fluorite structure which consists of the corner-shared CeO<sub>7+x</sub> hexahedrons forming the backbone of the network and La<sup>3+</sup> ions substituting Ce<sup>4+</sup> sites; there is a big hole formed via eight CeO<sub>7+x</sub> hexahedrons [10]. It can

mainly stand vacancies at the La<sup>3+</sup>, Ce<sup>4+</sup>, and O<sub>2</sub> sites without phase transformation. When La<sub>2</sub>Ce<sub>2</sub>O<sub>7</sub> nanoparticles participate in PVA matrix, the vacancies to cause water transfer in nanocomposite membranes. Hence the nanoparticles raise the proton conductivity. Both La<sup>3+</sup> and Ce<sup>4+</sup> can be substituted by many other elements with comparable ionic radii when the electrical neutrality is satisfied, which provides the possibility of tailoring its thermal properties [11]. A cubic fluorite structure is stable without phase transformation even after long-term annealing at 1673 K [12].

The aim of this study is preparation of new nanocomposite PEMs with high proton conductivity. To achieve this aim, PVA/ La<sub>2</sub>Ce<sub>2</sub>O<sub>7</sub> (PVA-LC) nanocomposite membranes were prepared via solution casting method. The effect of the La<sub>2</sub>Ce<sub>2</sub>O<sub>7</sub> nanoparticles on the water uptake, proton conductivity and fuel cell performance of PVA/ La<sub>2</sub>Ce<sub>2</sub>O<sub>7</sub> nanocomposite membranes for use in PEM fuel cells was investigated.

---

## 2. Experimental

### 2.1. Materials

The PVA from Mearck (99% hydrolyzed, average MW=145,000) was used as the backbone polymer matrix. The cross-linking agent was a 25 wt. % solution of glutaraldehyde (GA) in water and purchased from Merck. Distilled deionised (DI) water was used through all experiments. La<sub>2</sub>Ce<sub>2</sub>O<sub>7</sub> nanoparticles with a particle size range of 48 to 70 nm were synthesized through a sol gel process [13] and used as modifier.

### 2.2. Preparation of membranes

The PVA-based membranes were obtained by dissolving appropriate amounts of PVA and La<sub>2</sub>Ce<sub>2</sub>O<sub>7</sub> nanoparticles, in DI water under stirring at 80 °C. The resulting solution was stirred continuously at 80 °C until becoming homogeneous and viscous. Then GA was gradually added. The well-mixed solution was

transferred to petri-glass dishes and the water was evaporated at room temperature. When visually dry, the membrane was dislodged from the petri-glass dishes easily. The prepared nanocomposite membranes were then stored in DI water to be kept hydrated for other process. PVA-LC<sub>x</sub> nanocomposite membranes were named for x wt. % of the nanoparticles.

### 2.3. Characterization techniques

Autolab PGSTAT303N Potentiostat-Galvanostat Impedance Analyzer (Ecochemie) was used to obtain the proton conductivity of the membranes under an oscillation potential of 5 mV from 100 Hz to 1 MHz. The sample membrane was immersed in DI water for 24 h at room temperature and then sealed between two platinum plates electrodes. The measurements were carried out on the potentiostatic mode. The resistance of the membrane was obtained from the high-frequency intercept of the impedance. The proton conductivity values were calculated by consuming the equation ( $\sigma = L/RS$ ), where,  $\sigma$ , L, R, S respectively refer to, proton conductivity (S/cm), thickness (cm), resistance from the impedance data ( $\Omega$ ) and cross-sectional area (cm<sup>2</sup>) of the membranes. The water uptake of the PVA nanocomposite membranes was calculated by measuring the change in weight before and after hydration. The membranes were submerged in DI water for 24 h. Then surface-attached water on the membranes was rubbed with paper and the wetted membranes weight ( $W_{\text{wet}}$ ) was determined. The weight of the dry membranes ( $W_{\text{dry}}$ ) was determined after drying them in a vacuum oven at 60 °C. The water uptake was intended by the following equation (1).

$$\text{Water uptake\%} = \frac{W_{\text{wet}} - W_{\text{dry}}}{W_{\text{dry}}} \times 100 \quad (1)$$

The FT-IR ATR spectra (600-4000 cm<sup>-1</sup>, resolution 4 cm<sup>-1</sup>) were recorded with a Bruker Equinox 55 using an attenuated total reflectance (ATR, single reflection) accessory purged with ultra dry compressed air. The morphology of nanocomposite membranes was investigated by using a Scanning electron microscopy

(SEM), (JSM-5600, Jeol Co.), coupled with energy dispersive x-ray (EDX) spectroscopy. The samples were freeze-fractured in liquid N<sub>2</sub> and coated with gold plate before SEM observations were carried out. For determining mechanical properties at first membranes were dried and then mechanical properties of the prepared membranes were measured by using Zwick/Roell Z030 tensile test machine. All the membranes were cut to the standard shape and all tests were performed at a crosshead speed of 10 mm/min and room temperature.

The catalyst slurry ink of the anode and cathode was prepared by using Pt-C (20 %), 15 wt.% Nafion binder solution (Aldrich), and a suitable amount of DI water and IPA. The resulting Pt-C inks were first ultrasonicated for 1 h. The Pt-C inks were loaded onto the carbon paper (Toray TGP-H-090) by a painting method to achieve a loading of 0.5 mg cm<sup>-2</sup>. The prepared electrodes were dried in a vacuum oven at 120 °C for 1 h. Membrane electrode assembly (MEA) with an active area of 5 cm<sup>2</sup> was obtained by hot pressing the cathode and anode sandwiched with the PVA-LC nanocomposite membrane at 25 °C under 100 kgf cm<sup>-2</sup> for 15 min. The flow rates for both hydrogen and oxygen gases were kept as 200 ml/min and 500 ml/min respectively. Polarization curves were obtained using a fuel cell evaluation system (FCT-150s).

## 3. Results and Discussion

### 3.1. FT-IR ATR spectra

Figure 1 indicates a typical FT-IR ATR spectra measured for PVA and PVA-LC<sub>4</sub> nanocomposite membranes. The broad bands at around 3200-3600 cm<sup>-1</sup> were assigned due to hydrogen bonding and -OH single vibration. The peak around 2850 cm<sup>-1</sup> was ascribed the presence of such free aldehyde groups [14]. The peak at 1720-1730 cm<sup>-1</sup> was detected the presence of such free C=O groups, but was apparently covered by vicinity band in this region. The peak at 1000 cm<sup>-1</sup> was assigned to the

C-O groups of PVA based membrane. The low intensity of the O-H peak ( $3258\text{ cm}^{-1}$  and  $3274\text{ cm}^{-1}$ ), due to better cross-linking of PVA with GA, was also

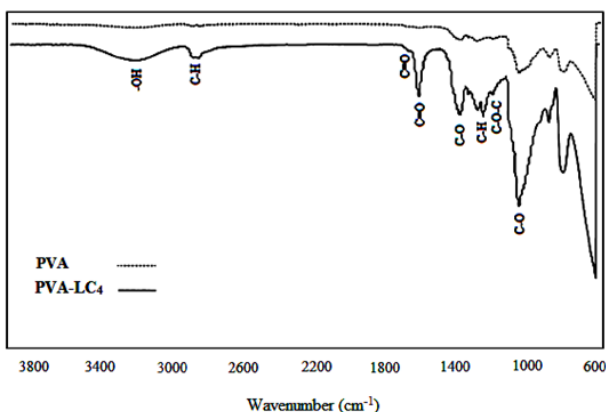


**Fig. 1.** FT-IR ATR spectra of PVA and PVA-LC<sub>4</sub> nanocomposite membranes.

clearly detected the presence of such free C=O groups, but was apparently covered by vicinity band in this region. The peak at  $1000\text{ cm}^{-1}$  was assigned to the C-O groups of PVA based membrane. The low intensity of the O-H peak ( $3258\text{ cm}^{-1}$  and  $3274\text{ cm}^{-1}$ ), due to better cross-linking of PVA with GA, was also clearly detected. The bands at  $1250\text{--}1270\text{ cm}^{-1}$  were ascribed to the ether bonds (C-O-C) between the -OH along the polymer chain of PVA with -CHO in GA [14]. The peaks at  $2907\text{ cm}^{-1}$  and  $1419\text{--}1421\text{ cm}^{-1}$  were apportioned to the C-H and C-O groups respectively.

### 3.2. Water uptake and proton conductivity

It is significant to know that the water uptake of the membranes is key factors which powerfully affect the proton conductivity of membranes. The protons can be transported in the hydrogen-bonded ionic network within fully water-swollen membranes.

PVA-LC nanocomposite membranes demonstrated higher water uptake and proton conductivity compared with PVA based membrane. The proton conductivity of pristine PVA membrane was found to be only  $\sim 1.0 \times 10^{-5}\text{ S/cm}$ . From the water uptake and proton conductivity results obtained, it can be concluded that incorporation of  $\text{La}_2\text{Ce}_2\text{O}_7$  nanoparticles in the PVA matrix, due to their hydrophilic nature, enhances

water uptake and proton conductivity properties of PVA membrane. The increase in the proton conductivity of the PVA-LC nanocomposite membranes is also related with the conductive network containing water- $\text{La}_2\text{Ce}_2\text{O}_7$  nanoparticles. These results can be explained due to hydrophilic character of the  $\text{La}_2\text{Ce}_2\text{O}_7$  nanoparticles.

$\text{La}_2\text{Ce}_2\text{O}_7$  nanoparticles with a cubic fluorite structure have vacancies at the  $\text{La}^{3+}$ ,  $\text{Ce}^{4+}$ , and  $\text{O}_2$  sites [10]. When  $\text{La}_2\text{Ce}_2\text{O}_7$  nanoparticles participate in PVA matrix, the vacancies lead to water transfer in the nanocomposite membranes and hence the proton conductivity increases. Proton transfer mechanism in PVA-LC nanocomposite membranes is demonstrated in Figure 2. As shown, the oxygen vacancy caused by La ion occupies the NNN (next nearest neighbor position) position of La ion, oxygen ion in adsorbed water molecule occupies the oxygen vacancy in the

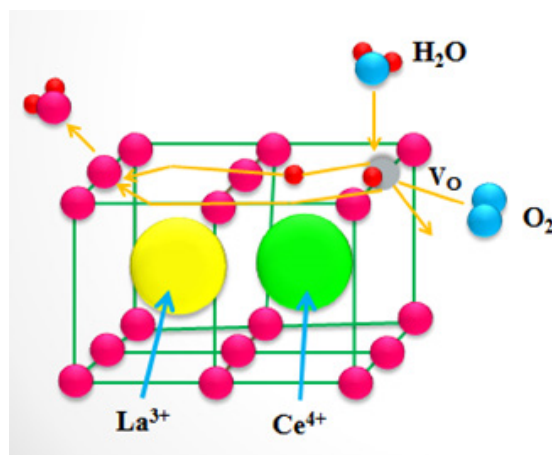


**Fig. 2.** Schematic description of defect configuration in  $\text{La}_2\text{Ce}_2\text{O}_7$  nanoparticles and water incorporation into oxygen vacancies in NNN position of La ions.

neighbor of Ce ions. At the similar time, two protons are formed close to this oxygen ion. These protons undergo electrostatic repulsion from central cation ( $\text{Ce}^{4+}$  or  $\text{La}^{3+}$ ). The repulsion between  $\text{La}^{3+}$  and proton is less than that between  $\text{Ce}^{4+}$  and proton, these protons have higher attraction to the La ions so they move to the oxygen ions in NN (nearest neighbor) positions. This process is shown in Figure 2 [15]. The quantum mechanical calculation results of Andersson et al. [16]

proposed that oxygen vacancies formation energy in next nearest neighbor position (NNN) of La ion is less than that in the nearest neighbor (NN) position.

Figure 3 shows typically the effect of  $\text{La}_2\text{Ce}_2\text{O}_7$  nanoparticles percent on the water uptake and proton conductivity of PVA-LC nanocomposite membranes. As shown in Figure 3, the proton conductivity of the nanocomposite membranes was increased with increase in nanoparticles content. It was revealed that PVA-LC<sub>4</sub> nanocomposite membranes demonstrated high water uptake (148%) and proton conductivity (0.019S/cm) compared with other PVA-LC nanocomposite membranes (Table 1).

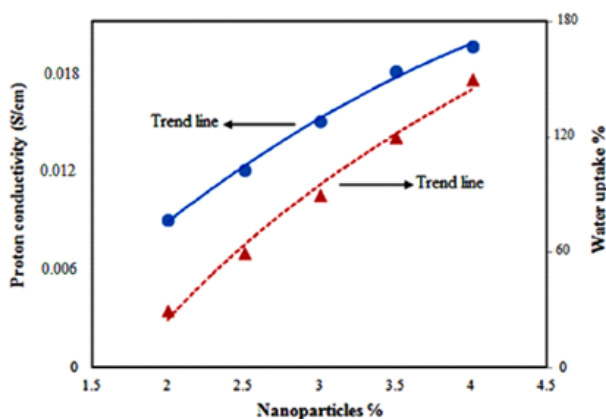


Fig. 3. Water uptake and proton conductivity plots of PVA-LC nanocomposite membranes.

Table 1. Specification of synthesized PVA membranes in 25 °C.

Membranes	Water uptake %	Proton conductivity (S/cm)	Elongation at break (%)	Tensile strength (MPa)
PVA-LC <sub>4</sub>	148	0.019	5.26	29.35
PVA	130	$5.01 \times 10^{-2}$	5.23	25.29

hydrated state. Figure 4(a) shows that PVA-LC<sub>4</sub> nanocomposite membranes have the lowest resistance (highest proton conductivity) compared with other nanocomposite membranes. Bode Modulus plots (Figure 4(b)) confirm the results, obtained from the Nyquist plots, which showed lower resistance for PVA-LC<sub>4</sub> nanocomposite membrane corresponds to the Nyquist plots.

### 3.3. Nanocomposite membrane morphology (SEM and EDX measurements)

Figure 5 shows the SEM images of PVA-LC<sub>4</sub> nanocomposite membranes. Apparently, SEM results confirmed the homogeneity of these nanocomposite membranes.

Energy dispersive X-ray spectroscopy established the existence of  $\text{La}_2\text{Ce}_2\text{O}_7$  nanoparticles in the composite

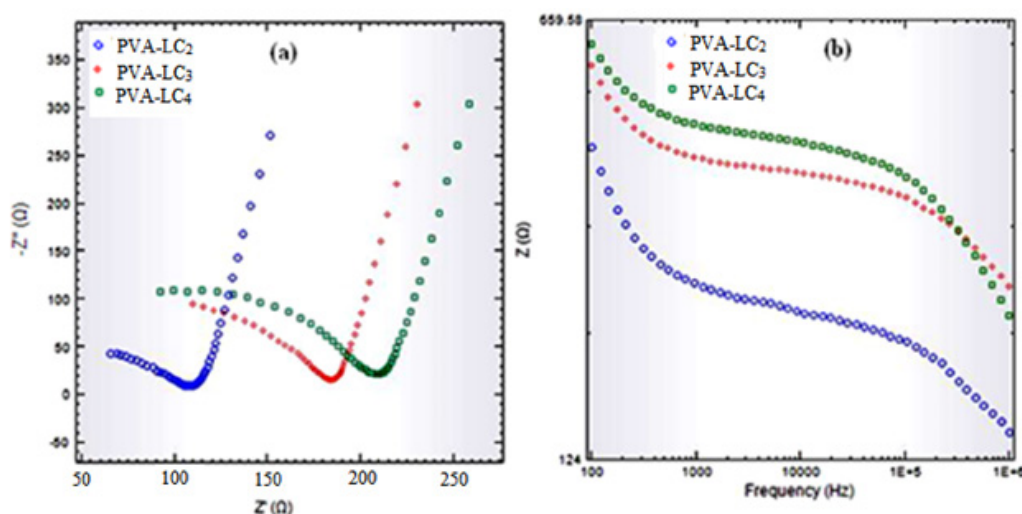


Fig. 4. Nyquist (a) and Bode Modulus (b) plot of PVA-LC nanocomposite membranes.

Figure 4 demonstrates Nyquist and bode modulus plots of PVA-LC nanocomposite membranes at fully

membranes. EDX distribution of nanoparticles in the cross-section of PVA-LC<sub>4</sub> nanocomposite membranes



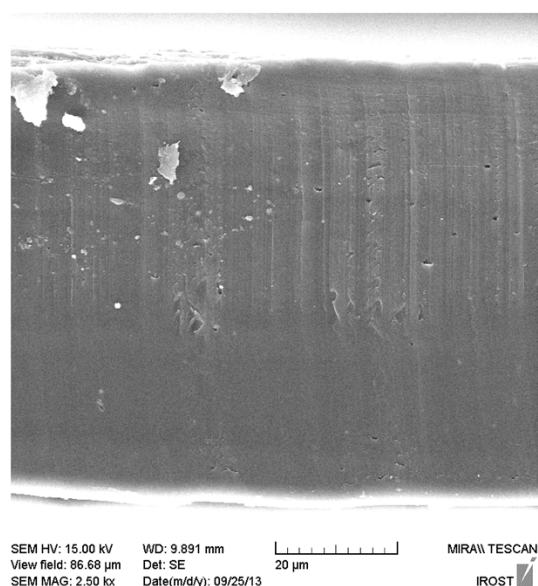


Fig. 5. SEM images of the PVA-LC<sub>4</sub> nanocomposite membranes.

is exhibited in Figure. 6. A homogenous distribution of La and Ce nanoparticles in the cross-section of PVA-LC<sub>4</sub> nanocomposite membranes was detected. The uniform distribution of La and Ce nanoparticles in PVA-LC<sub>4</sub> nanocomposite membranes increases the proton transfer in cubic fluorite structure of La<sub>2</sub>Ce<sub>2</sub>O<sub>7</sub> nanoparticles.

### 3.4. Mechanical properties

From Table 1 it was found that the nanocomposite

membranes due to strong interactions of La<sub>2</sub>Ce<sub>2</sub>O<sub>7</sub> nanoparticles with PVA based membrane, displayed a higher mechanical stability than PVA based membrane. La<sub>2</sub>Ce<sub>2</sub>O<sub>7</sub> nanoparticles have excellent mechanical stability and increase a mechanical stability of PVA-LC<sub>4</sub> nanocomposite membranes when incorporated in PVA matrix. EDX distribution demonstrated homogenous distribution of La and Ce nanoparticles in the PVA-LC<sub>4</sub> nanocomposite membranes (Figure. 6). Uniform dispersion of nanoparticles in the PVA-LC<sub>4</sub> nanocomposite membranes, which increases the PVA-nanoparticles interactions, plays also a key role in improvement of its mechanical stability. PVA-LC<sub>4</sub> nanocomposite membranes are adequate to be fabricated into membrane electrode assemblies.

### 3.5. Electrochemical measurements

The PVA-LC nanocomposite membranes were used for their performance assessment in H<sub>2</sub>/O<sub>2</sub> PEM fuel cells by MEAs. The catalyst loading on both the anode and the cathode (active area = 5 cm<sup>2</sup>) was kept at 0.5 mg cm<sup>-2</sup>.

Figure 7 depicts i-V and power density curves for the PEM fuel cells using PVA-LC nanocomposite membranes at 25 °C. The maximum power density of 9.5 mW/cm<sup>2</sup> with a peak current density of 58 mA/cm<sup>2</sup> was obtained for PVA-LC<sub>2</sub> nanocomposite membranes at 25 °C. This peak was shifted to higher current (130 mA/cm<sup>2</sup>) with a higher power density (19 mW/

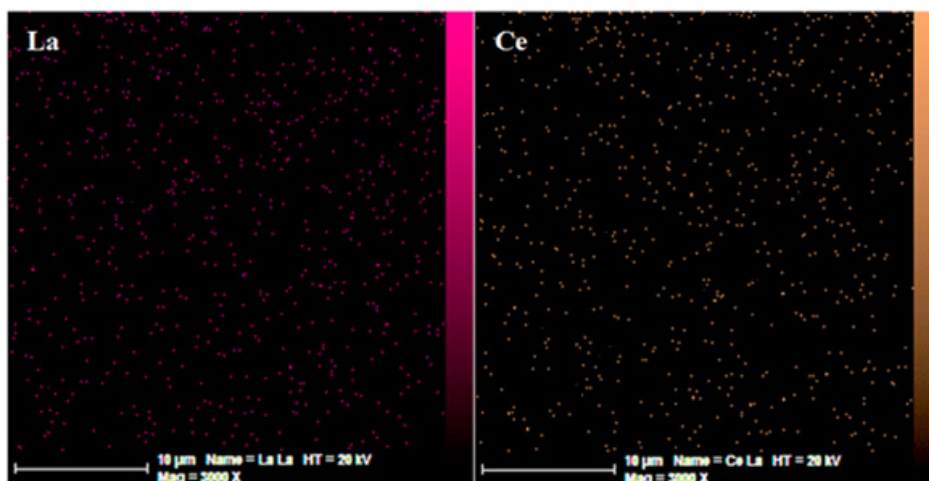
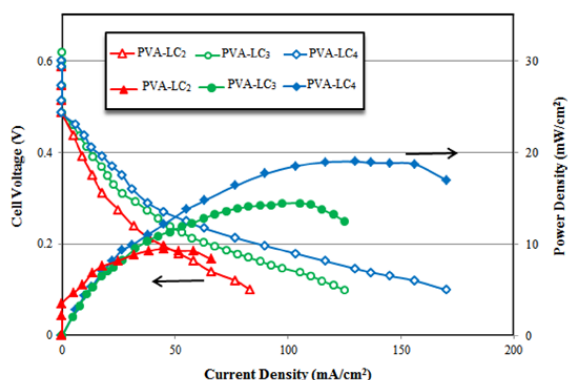


Fig. 6. EDX analysis of the PVA-LC<sub>4</sub> nanocomposite membranes cross-section.



**Fig. 7. Comparison of i-V and Power Density curves for the PEM fuel cells using PVA-LC nanocomposite membranes. The cell temperature is at 25 °C with ambient pressure. The anode and cathode Pt loadings were both 0.5 mg cm<sup>-2</sup>. Each MEA with an active area of 2.3×2.3 cm<sup>2</sup> was performed the fuel cell test with the H<sub>2</sub>/O<sub>2</sub> flow rates at 300/500 mL min<sup>-1</sup>.**

cm<sup>2</sup>) with increasing a nanoparticles content for PVA-LC<sub>4</sub> nanocomposite membranes.

The open-circuit voltage (OCV) is determined when no current flows into the fuel cell. This is known as the initial voltage prior to the cell voltage measurement. The open circuit voltage detected for PVA-LC<sub>4</sub> nanocomposite membranes in 25 °C was about 0.62 V.

#### 4. Conclusions

PVA-La<sub>2</sub>Ce<sub>2</sub>O<sub>7</sub> nanocomposite membranes were prepared with solutions casting method. Glutaraldehyde (GA) was used as cross linking agent. The significant improvement has been achieved via the synergetic combination of organic and inorganic phases. Nanocomposite membranes were structurally and morphologically considered by FT-IR and SEM. All of the nanocomposite membranes due to vacancies at the La<sup>3+</sup>, Ce<sup>4+</sup>, and O<sub>2</sub> sites in La<sub>2</sub>Ce<sub>2</sub>O<sub>7</sub> nanoparticles displayed higher water uptake and proton conductivity than that of the PVA membrane. SEM images displayed a homogeneous dispersion of nanoparticles in the nanocomposite membranes. The PVA-La<sub>2</sub>Ce<sub>2</sub>O<sub>7</sub> nanocomposite membranes showed a high proton conductivity and water uptake.

The maximum current densitie of 170 mA/cm<sup>2</sup> was found at 25 °C for the PVA -La<sub>2</sub>Ce<sub>2</sub>O<sub>7</sub> nanocomposite membranes. The proposed composite membrane is a viable candidate for PEM fuel cells applications.

#### 5. References

1. Andujar J, Segura F, "Fuel cells History and updating. A walk along two centuries, "Renewable and Sustainable Energy", 2009, 13: 2309.
2. Diaz M, Ortiz A, Vilas M, Tojo E, Vilas M, Ortiz I, "Performance of PEMFC with new polyvinyl-ionic liquids based membranes as electrolytes", Int. J. Hydrogen Energy, 2014, 39: 3970.
3. Thanganathan U, Parrondo J, Rambabu B, "Nanocomposite hybrid membranes containing polyvinyl alcohol or poly(tetramethylene oxide) for fuel cell applications", J. Appl. Electrochem, 2011, 41: 617.
4. Wu Y, Wu C, Li Y, Fu Y, "PVA-silica anion-exchange hybrid membranes prepared through a copolymer crosslinking agent", J. Membr. Sci, 2010, 350: 322.
5. Xu W, Liu C, Xue X, Su Y, Lv Y and Xing W, "New proton exchange membranes based on poly (vinyl alcohol) for DMFCs", Solid State Ionics, 2004, 171: 121.
6. Yang CC and Lee YJ, "Preparation of the acidic PVA/MMT nanocomposite polymer membrane for the direct methanol fuel cell (DMFC)", Thin Solid Films, 2009, 517: 4735.
7. Beydaghi H, Javanbakht M, Salar Amoli H, Badiei H, Khaniani Y and Ganjali MR, "Synthesis and characterization of new proton conducting hybrid membranes for PEM fuel cells based on poly (vinyl alcohol) and nanoporous silica containing phenyl sulfonic acid", Int. J. Hydrogen Energy, 2010, 36: 13310.
8. Salarizadeh P, Javanbakht M, Abdollahi M and Najji L, "Preparation, characterization and properties of

- proton exchange nanocomposite membranes based on poly(vinyl alcohol) and poly(sulfonic acid)-grafted silica nanoparticles”, *Int. J. Hydrogen Energy*, 2013, 38: 5473.
9. Hooshyari Kh, Javanbakht M, Naji L and Enhessari M, “Nanocomposite proton exchange membranes based on Nafion containing  $\text{Fe}_2\text{TiO}_5$  nanoparticles in water and alcohol environments for PEMFC”, *J. Membr. Sci*, 2014, 454: 74.
10. Litao Y, Wenping S, Lei B, Shumin F, Zetian T and Wei L, “Effect of Sm-doping on the hydrogen permeation of  $\text{Ni-La}_2\text{Ce}_2\text{O}_7$  mixed protonic electronic conductor”, *Int. J. Hydrogen Energy*, 2010, 35: 4508.
11. Wen M, Shengkai G, Huibin X and Xueqiang C, “On improving the phase stability and thermal expansion coefficients of lanthanum cerium oxide solid solutions”, *Scripta Mater*, 2006, 54: 1505.
12. Xu Z, He L, Mu R, He S, Huang G and Cao X, “Double-ceramic-layer thermal barrier coatings based on  $\text{La}_2(\text{Zr}_{0.7}\text{Ce}_{0.3})_2\text{O}_7/\text{La}_2\text{Ce}_2\text{O}_7$  deposited by electron beam-physical vapor deposition”, *Appl. Surf. Sci*, 2010, 256: 3661.
13. Enhessari M, Ozaee K, Shaterian M and Karamali E, “Strontium cerate nanoparticle synthesis method”, US Patent 512 654.
14. Qiao J, Hamaya T and Okada T, “New highly proton-conducting membrane poly(vinyl pyrrolidone)(PVP) modified poly(vinyl alcohol)/2-acrylamido-2-methyl-1-propanesulfonic acid (PVA-PAMPS) for low temperature direct methanol fuel cells (DMFCs)”, *Polym. J*, 2005, 46: 10809.
15. Zuo CD, Lee TH, Song SJ, Chen L, Dorris SE and Balachandran U, “Hydrogen permeation and chemical stability of cermet Ni-Ba  $[\text{Zr}_{0.8x}\text{Ce}_x\text{Y}_{0.2}]_3\text{O}_3$  Membranes”, *Electrochem Solid State Lett*, 2005, 8: 35.
16. Andersson D, Simak, Skorodumova Natalia N, AbrikosovIgor A, Johansson B, “Optimization of ionic conductivity in doped ceria”, *Proc Natl Acad Sci USA*, 2006, 103: 3518.